



ELSEVIER

Available online at [www.sciencedirect.com](http://www.sciencedirect.com)



Journal of Magnetism and Magnetic Materials 293 (2005) 589–596



[www.elsevier.com/locate/jmmm](http://www.elsevier.com/locate/jmmm)

# An immunomagnetic separator for concentration of pathogenic micro-organisms from large volume samples

Ovidiu Rotariu<sup>a,b,\*</sup>, Iain D. Ogden<sup>c</sup>, Marion MacRae<sup>c</sup>, Vasile Bădescu<sup>b</sup>,  
Norval J.C. Strachan<sup>a</sup>

<sup>a</sup>*School of Biological Sciences, University of Aberdeen, Cruickshank Building, St. Machar Drive, Aberdeen, UK*

<sup>b</sup>*National Institute of R-D for Technical Physics I.F.T. Iași, Mangeron 47 Blvd., Iași, România*

<sup>c</sup>*Department of Medical Microbiology, University of Aberdeen, Aberdeen, UK*

Available online 4 March 2005

## Abstract

The standard method of immunomagnetic separation of pathogenic bacteria from food and environmental matrices processes 1 ml volumes. Pathogens present at low levels (<1 pathogenic bacteria per ml) will not be consistently detected by this method. Here a flow through immunomagnetic separator (FTIMS) has been designed and tested to process large volume samples (>50 ml). Preliminary results show that between 70 and 113 times more *Escherchia coli* O157 are recovered compared with the standard 1 ml method.

© 2005 Published by Elsevier B.V.

**Keywords:** Immunomagnetic separation; Magnetic particles; Pathogenic micro-organisms; *E. coli* O157; Mathematical modeling; Food pathogens

## 1. Introduction

Immunomagnetic separation (IMS) is an established technique that involves application of antibody coated magnetic particles (MPs) to separate pathogenic micro-organisms, biological cells or chemical compounds from clinical, food, soil, fecal and environmental samples [1–3]. In the microbiological analysis of food, the ingestion of low

numbers (<10) of pathogens may lead to food poisoning [4] thus necessitating application of separation systems (e.g. IMS) to concentrate the target micro-organisms.

Current standard IMS devices use 1–8 μm MPs to test volumes of 1 ml [5]. This may be a problem when testing samples containing low numbers of target organisms. Attempts have been made to increase the sample size to 10 ml, which resulted in a 7-fold increase in sensitivity [6]. Increasing the sample size further (e.g. to >50 ml) could dramatically increase the sensitivity of the IMS process.

\*Corresponding author. School of Biological Sciences, University of Aberdeen, Cruickshank Building, St. Machar Drive, Aberdeen, UK. Tel.: +44 1224 272256; fax: +44 1224 272703.

E-mail address: [o.rotariu@abdn.ac.uk](mailto:o.rotariu@abdn.ac.uk) (O. Rotariu).

This paper reports the specification, design and testing of a flow through immunomagnetic separator (FTIMS) for concentrating micro-organisms from large volume solutions (e.g. food homogenates > 50 ml). Results obtained from the FTIMS for concentrating *Escherichia coli* O157 from buffer and food samples are compared with standard small volume IMS techniques.

## 2. Design specification

A specification of what is needed in the microbiology laboratory was prepared. The main requirements were:

- The ability to process samples > 50 ml volume,
- Individual samples should be processed within 30 min,
- Simultaneous processing of multiple samples (e.g. 8),
- Final sample volume of 1 ml,
- At least 10-fold increase of sensitivity compared with the standard method,
- Equipment must be user friendly, robust and easy to keep sterile,
- Suitable for use with commercially available MPs.

## 3. Design of the flow through immunomagnetic separator

A flow through system was chosen because static magnetic separation in large volume systems is not practical. The flow through system was designed using a high magnetic field with medium gradient, which should be sufficient for capturing the MPs in a standard silicone tube (~2 mm inner diameter).

The main element of the FTIMS system is the separation cell (Fig. 1a). It consists of a ferromagnetic wire magnetised in a uniform background magnetic field. Magnetisation of the wire enables generation of a high magnetic force allowing the MP and cell aggregates to be captured on the tube wall. The FTIMS system (Fig. 1b) has as input a biological sample to be processed (1) which

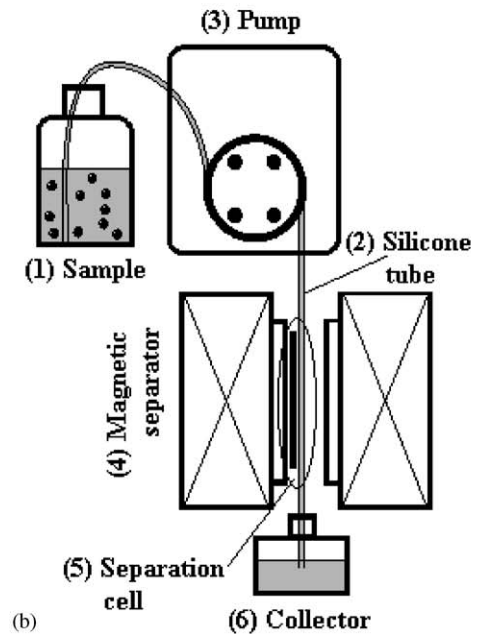
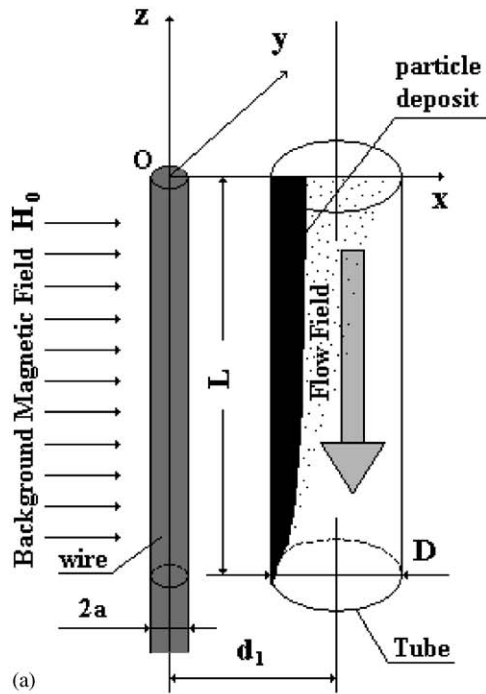


Fig. 1. (a) Separation cell that consists of a ferromagnetic wire of length  $L$  and radius  $a$ , magnetised in a uniform background magnetic field of intensity  $H_0$ . The ferromagnetic wire is aligned along the  $z$ -axis, at a distance  $d_1$  from the central axes of a silicone tube of inner diameter  $D$ . (b) Schematic diagram of FTIMS.

consists of a mixture of cells or microbes (e.g. *E. coli* O157 and bacterial flora) suspended in a carrier liquid (e.g. beef mince homogenate). The sample is mixed and incubated with specific antibody coated MPs (e.g. IDG LabM anti-*E. coli* O157 coated MPs, UK) for selective immunosorption of the bacterial target cells. Then, the broth is passed through a silicone tube (2) using a peristaltic pump (3) to the magnetic separator (4), in the presence of a high magnetic field. The MPs together with the attached cells remain attached on the tube wall in the region adjacent to the separation cell (5). The remaining suspension passes through to the collection chamber (6). The captured product is cleaned, the magnetic field is switched-off and the particles are collected in a separate test tube.

### 3.1. Quantifying the FTIMS system parameters by simulation

In order to achieve in practice a final sample volume  $<1$  ml the inner diameter of the silicone tube must be  $D < 5$  mm and the length of the tube in the active magnetic space  $L < 5$  cm. To process samples up to 250 ml within 30 min the flow rate must be  $Q \sim 10$  ml/min. Using tubes with an inner diameter between  $2 \text{ mm} < D < 5 \text{ mm}$  requires the mean flow velocity  $v_0$  of the suspension to lie between  $0.8 \text{ cm/s} < v_0 < 5.5 \text{ cm/s}$ . Previous magnetic separation work [7] shows that such a system is possible for magnetic fields  $H_0 > 500\,000$  A/m, flow velocities of  $v_0 \sim 1.0$  cm/s and magnetic wires of radius  $a \sim 1.0$  mm.

In order to determine the appropriate FTIMS system parameters (Table 1) two numerical methods were used. The first was the 2D “Finite Element Method Magnetics” program (FEMM3.2) from Foster-Miller (<http://femm.foster-miller.com>), which was used to simulate the magnetic field in the separation device. The second numerical method was performed in Mathematica 5.0 (Wolfram Research, USA) and calculated the capture of the particle-pathogen aggregates by solving the equations describing their trajectories. Table 1 shows the six parameters which were varied in computation in order to get best values: (i) the radius and the length of the wire—are

important for the dimension of the system; (ii) the intensity of the magnetic field, the flow rate/fluid velocity and the MPs size—are the process parameters which are easy to change in practice. Table 1 also denotes the fixed values of the other system parameters.

(a) *The estimation of the radius of the ferromagnetic wire*: The radius of the wire is the parameter that influences the volume of space on which the gradient of the magnetic field is highest resulting in attraction of MPs to the wire. The magnetic field profile was modelled for wires of various radii and intensity of the magnetic field. Fig. 2 presents the 2D map of the magnetic field (Fig. 2a) and the variation of its intensity (Fig. 2b) when the radius of wire is  $a = 1.6$  mm. The density of the flux lines and the values of the magnetic field (dark grey—higher values of the magnetic field), show that magnetic field is most intense in the direction of magnetisation of the wire ( $Ox$ ) at  $y = 0$ . The gradient of the magnetic field around the wire is highest at a range (measured from wire’s surface) of approximately three times the radius of the wire. This is the useful space expected to be used for the magnetic capture process, where the magnetic attractive force is largest. Using wires with radii between  $1.5 \text{ mm} < a < 2.0 \text{ mm}$  the highest gradient of the magnetic field encompasses up to 6 mm on  $x$  and  $y$  directions, which includes the space occupied by tubes with outer diameters  $< 5$  mm.

(b) *The estimation of the length of the separation cell (wire)*: Long separation cells will ensure greatest capture of particles. However, the volume of tube that these MPs will be captured in would be large (e.g.  $> 1$  ml). Hence, it is important to minimise the length of the wire (separation cell) but also to ensure high capture recovery of MPs. To estimate the length of the separation cell the trajectory of the MPs and micro-organisms aggregates (MP–Mo) as they move along the tube must be calculated. If the length of the separation cell,  $L >$  capture length (the length of trajectory’s projection on flow direction,  $Oz$ ) the recovery of MP–Mo aggregates is 100%. Taking into account the magnetic and drag forces that act on MP–Mo aggregates, their equations of motion are deduced as described for a single paramagnetic particle in a

Table 1

Parameters used to design and test FTIMS—final column gives the recommended parameter values after accomplishing the experiments

Parameter	Values used in modeling	Appropriate value estimated in modelling	Values used in experiments	Recommended FTIMS parameter values
Wire's radius $a$ (mm)	1–3.0	1.5–2 (Fig. 2)	1.6	1.5–2
Wire's length (capture length) $L$ (cm)	Free	<6 (Figs. 3 and 4)	3.7	3.5–5
Wire's magnetisation of saturation $M_{\text{wire}}$ (A/m)	$12 \times 10^5$	N.A.	$12 \times 10^5$	$12 \times 10^5$ – $16 \times 10^5$
Tube's inner diameter $D$ (mm)	2.4	N.A.	2.4	2–3
Tube's outer diameter (mm)	4.0	N.A.	4.0	4–5
Distance wire-tube $d_1$ (mm)	3.6	N.A.	3.6	Wire in touch with the tube
MPs's diameter $d_{\text{MP}}$ ( $\mu\text{m}$ )	1–4	>2	0.8–8	2–8
MP's magnetisation $M_{\text{MP}}$ (A/m)	< 135 000 (30% $\text{Fe}_3\text{O}_4$ w/w)	N.A.	N.A. (29–33% $\text{Fe}_3\text{O}_4$ w/w)	> 130 000
Micro-organism's size $d_{\text{Mo}}$ ( $\mu\text{m}$ )	1	N.A.	N.A.	N.A.
Intensity of magnetic field $H_0$ (A/m)	160 000–960 000	> 500 000 (Fig. 4)	80 000–640 000	> 600 000 for $L > 3.7$ cm (Fig. 5)
Flow rate $Q$ (ml/min)	5–10	<7	7–10	< 7 for $D = 2.4$ mm (Fig. 5)
Flow velocity $v_0$ (cm/s)	1.85–3.70	<3.70	2.58–3.70	< 2.58 for $D = 2.4$ mm
Viscosity of fluid $\eta_f$ ( $\text{kg m}^{-1} \text{s}^{-1}$ )	0.001	N.A.	0.001	0.001
Magnetic permeability of free space $\mu_0$ (H/m)	$4\pi \times 10^{-7}$	N.A.	N.A.	N.A.
Number of MPs /aggregate $n_{\text{MP}}$	1	N.A.	N.A.	N.A.
Number of micro-organisms/aggregate $n_{\text{Mo}}$	1	N.A.	N.A.	N.A.
Pole diameter (cm)	N.A.	N.A.	3.7	3.5–5

N.A.—Not applicable.

high gradient magnetic field [8]. Briefly,

$$\frac{dx_a}{dt} = \frac{v_m}{a} \frac{\partial \sqrt{h_x^2 + h_y^2}}{\partial x_a}, \quad (1a)$$

$$\frac{dy_a}{dt} = \frac{v_m}{a} \frac{\partial \sqrt{h_x^2 + h_y^2}}{\partial y_a}, \quad (1b)$$

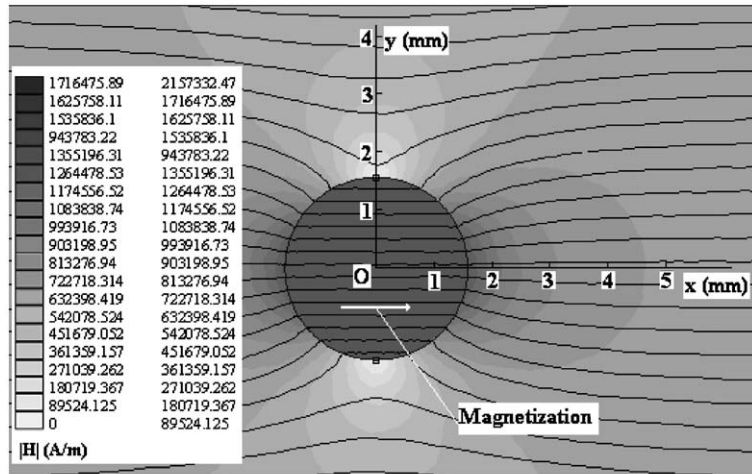
$$\frac{dz_a}{dt} = -\frac{v_0}{a}, \quad (1c)$$

where

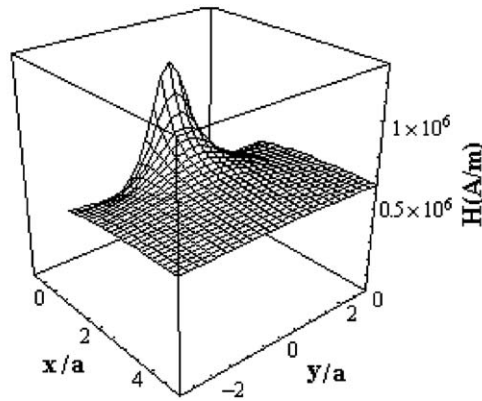
$$h_x = \frac{1}{K} + \left( \frac{(x/a)^2 - (y/a)^2}{((x/a)^2 + (y/a)^2)^2} \right), \quad (2a)$$

$$h_y = \frac{2(x/a)(y/a)}{((x/a)^2 + (y/a)^2)^2}, \quad (2b)$$

are terms which give the spatial dependence of the components of the magnetic field around the ferromagnetic wire. The “magnetic velocity” in



(a)



(b)

Fig. 2. (a) 2D map of the magnetic field calculated in a plane perpendicular to the ferromagnetic wire. (The parameters used in the simulation were: radius of wire  $a = 1.6$  mm, magnetisation of saturation  $M_{\text{wire}} = 1\,200\,000$  A/m, intensity of the background magnetic field  $H_0 = 640\,000$  A/m). Illustrated are the flux lines around the magnetised ferromagnetic wire and the intensity of the magnetic field  $H$  (dark grey—higher values). (b) 3D view of the intensity of the magnetic field.

Eq. (1a) and (1b) is given by [9]

$$v_m = \left( \frac{\mu_0 d_{\text{VMP-Mo}}^3 M_{\text{MP-Mo}} H_0 K}{18 \eta_f d_{\text{SMP-Mo}} a} \right). \quad (3)$$

This velocity is defined as the terminal velocity of the MP–Mo aggregates under the action of magnetic and drag forces. In Eq. (3)  $\mu_0$  is the magnetic permeability of free space,  $\eta_f$  the viscosity of fluid, and  $d_{\text{VMP-Mo}}$ ,  $d_{\text{SMP-Mo}}$  and  $M_{\text{MP-Mo}}$  are the volume diameter, the surface diameter and the magnetisation of the MP–Mo aggregates, respectively. Also,  $K$  is a dimensionless

constant dependent upon the magnetic properties of the ferromagnetic wire and the intensity of the magnetic field.  $K = M_{\text{wire}}/2H_0$  for a wire magnetised at saturation and  $K = 1$  when the wire is unsaturated.

The volume and hydrodynamic diameters of the aggregates are given by [10]:

$$d_{\text{VMP-Mo}} = \sqrt[3]{n_{\text{MP}} d_{\text{MP}}^3 + n_{\text{Mo}} d_{\text{Mo}}^3}, \quad (4)$$

$$d_{\text{SMP-Mo}} = \sqrt{n_{\text{MP}} d_{\text{MP}}^2 + n_{\text{Mo}} d_{\text{Mo}}^2}, \quad (5)$$

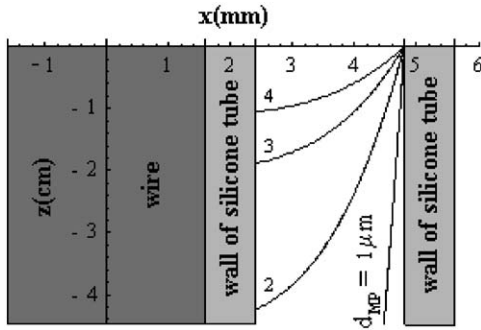


Fig. 3. Typical trajectories calculated by solving Eqs. (1) for MPs having various diameters:  $d_{MP} = 1, 2, 3$  and  $4 \mu\text{m}$ . (The remaining parameters used in simulation were:  $H_0 = 640\,000 \text{ A/m}$ ,  $K = 0.91$ ,  $Q = 10 \text{ ml/min}$  ( $D = 2.4 \text{ mm}$ ,  $v_0 = 3.70 \text{ cm/s}$ ),  $a = 1.6 \text{ mm}$ ,  $d_1 = 3.6 \text{ mm}$ ,  $\eta_f = 10^{-3} \text{ kg m}^{-1} \text{ s}^{-1}$ ,  $d_{Mo} = 1 \mu\text{m}$ ,  $n_{Mo} = 1$ ,  $n_{MP} = 1$  and maximum value of  $M_{MP} = 135\,000 \text{ A/m}$ ).

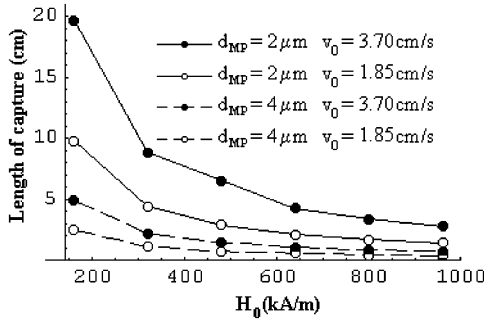


Fig. 4. Dependence of the length of capture vs. the intensity of background magnetic field  $H_0$  calculated using Eqs. (1). The diameter of MPs and the velocity of the fluid (flow rate) vary as shown ( $d_{MP} = 2 \mu\text{m}$ —full line;  $4 \mu\text{m}$ —dashed line;  $v_0 = 3.70 \text{ cm/s}$  ( $Q = 10 \text{ ml/min}$ )—full dot;  $v_0 = 1.85 \text{ cm/s}$  ( $Q = 5 \text{ ml/min}$ )—circle). The remaining parameters are kept constant and are the same as in Fig. 3 (excepting  $K$  that varies with  $H_0$ ,  $K \in (0.625, 1)$ ).

where  $d_{MP}$ ,  $n_{MP}$ ,  $d_{Mo}$ ,  $n_{Mo}$  are the diameters and the numbers of MPs and micro-organisms that aggregate and form a cluster.

The MP–Mo aggregates have magnetization given by

$$M_{MP-Mo} = M_{MP} \frac{1}{1 + (n_{Mo}d_{Mo}/n_{MP}d_{MP})^3}, \quad (6)$$

where  $M_{MP}$  is the magnetization of MPs and this varies with the magnetic field according with the Langevin law [11,12].

The trajectories of the MP–Mo aggregates under the action of the magnetic and hydrodynamic forces are calculated by numerically solving the differential equation of their motion (1) (Runge-Kutta of fourth order [13]). Examples of trajectories for a single MP–Mo aggregate ( $n_{MP} = 1$ ,  $n_{Mo} = 1$ ) are presented in Fig. 3, for MPs having diameters  $d_{MP} = 1, 2, 3$  and  $4 \mu\text{m}$ . It can be seen that the capture length decreases when the size of the MPs increases. Fig. 4 presents the dependence of the capture length on the intensity of background magnetic field, the velocity of the fluid (flow rate) and the size of particles. The maximum capture length is  $\sim 19.68 \text{ cm}$  for the weakest magnetic field, smaller magnetic particle and highest flow velocity ( $H_0 = 160\,000 \text{ A/m}$ ,  $d_{MP} = 2 \mu\text{m}$ ,  $v_0 = 3.70 \text{ cm/s}$ ) and  $\sim 0.37 \text{ cm}$  for the highest magnetic field, larger magnetic particle and lower flow velocity ( $H_0 = 960\,000 \text{ A/m}$ ,  $d_{MP} = 4 \mu\text{m}$ ,  $v_0 = 1.85 \text{ cm/s}$ ). But in practice only fields  $< 800\,000 \text{ A/m}$  are feasible at this size scale. Hence using a magnetic field in this range together with a ferromagnetic wire of radius  $a = 1.6 \text{ mm}$  and a tube with inner diameter  $D = 2.4 \text{ mm}$ , placed at a distance  $d_1 = 3.6 \text{ mm}$  from the wire's axis, it should be possible to obtain capture lengths of few centimetres ( $< 6 \text{ cm}$ ) suitable for the current application (other parameters of process are given in Table 1).

#### 4. Experimental results for the recovery of MPs

A separation cell based on the theoretical results above and detailed in Table 1 was mounted on a silicone tube (Tygon, Saint-Gobain, USA) inside the air gap of a type C electromagnet (Newport Instruments, UK). The length of the wire (the maximum capture length) was chosen as the poles diameter ( $3.7 \text{ cm}$ ), which is within the range of values predicted by the simulations. The intensity of the magnetic field was varied between  $80,000$  and  $640\,000 \text{ A/m}$  using a constant current power supply, and the flow rate was varied between  $7$  and  $10 \text{ ml/min}$  using a Miniplus2 peristaltic pump (Gilson, France).

The MPs (IDG LabM, Bury, UK) were suspended in either  $0.01 \text{ M}$  phosphate buffer saline



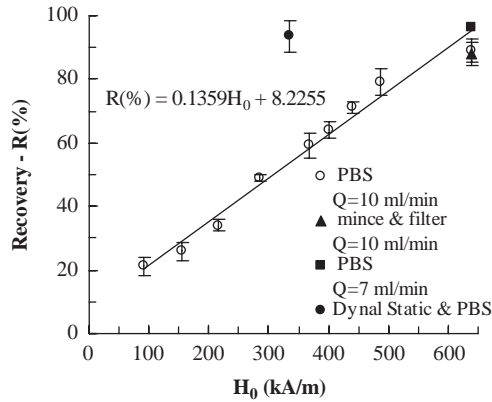


Fig. 5. Recovery of IDG LabM particles (diameter range 1–8  $\mu\text{m}$ ) vs. the intensity of background magnetic field  $H_0$  and flow rate  $Q$  using FTIMS:  $\circ$  PBS ( $Q = 10$  ml/min);  $\blacktriangle$  mince and filter ( $Q = 10$  ml/min);  $\blacksquare$  PBS ( $Q = 7$  ml/min).  $\bullet$  Reference recovery using the standard separator—Dynal Static and PBS (MPC-S 1 ml system).

(PBS) or filtered beef mince homogenate. The recovery of particles was determined either by the weighing method (the mass of particles recovered compared with the mass of particles in sample buffer/homogenate), or by optical counting (the ratio of the particle numbers recovered to that in the initial sample).

The mean recovery of the MPs (suspended in PBS) increased linearly with the magnetic field (Fig. 5). A maximum recovery of 89% has been obtained for  $H_0 = 640\,000$  A/m and a flow rate of  $Q = 10$  ml/min ( $v_0 = 3.70$  cm/s). This was repeated in beef homogenate previously filtered using a fine mesh filter (pore size  $< 100$   $\mu\text{m}$ ) (BagFilter P, M-Tech, UK). The recovery was found to be 88%. The reference recovery of MPs suspended in PBS for the standard separator (Dynal MPC-S 1 ml, Dynal, UK) is 93.5%. In order to obtain a higher recovery (i.e. similar to Dynal) the experiment was repeated in PBS using a magnetic field of intensity  $H_0 = 640\,000$  A/m and a lower flow rate  $Q = 7$  ml/min ( $v_0 = 2.58$  cm/s). The mean recovery of MPs was 96.2%. The 4% of particles lost was because of their small size ( $< 1.0$   $\mu\text{m}$ ). Preliminary tests using Dynal 2.8  $\mu\text{m}$ , and Dynal 4.5  $\mu\text{m}$  beads show a recovery  $> 98\%$  for the same conditions mentioned above (data not presented).

## 5. Comparison of FTIMS with standard Dynal 1 ml method

Preliminary IMS experiments were performed in PBS to which were added decimal dilutions of *E. coli* O157 cocktails (four separate strains) grown in nutrient broth for 18 h at 37 °C. Bacterial counts on each cocktail were performed by the modified Miles and Misra technique [14] on nutrient agar incubated at 37 °C. Volumes (0.5 ml) of the 1:100 000 ( $10^{-5}$ ) to 1:100 000 000 ( $10^{-8}$ ) dilutions were added separately to 50 ml volumes of sterile PBS. To each aliquot (50 ml) was added 0.05 ml Captivate™ O157 (IDG LabM, Bury, UK) immunomagnetic beads and mixed for 30 or 60 min on a flat bed shaker (300 rev/min) at room temperature. The sample was passed through FTIMS and the captured beads were re-suspended in 3 ml wash buffer (PBS + 0.05% Tween-20). Two further washing stages were performed prior to spreading each set of re-suspended beads (100  $\mu\text{l}$ ) equally onto two cefixime tellurite sorbitol MacConkey plates. After overnight incubation at 37 °C, the number of non-sorbitol-fermenting target colonies (confirmed as *E. coli* O157 by latex agglutination (Oxoid)) were counted. The number of colonies on the duplicate plates are added together and presented as a function of decimal dilution. These are compared with the 1 ml standard Dynal separator and also the 10 ml Dynal separator (Fig. 6). Significantly more colonies were detected by using FTIMS when compared with the Dynal separators. The mean number of colonies detected for  $10^{-5}$  dilution were 113-fold higher using FTIMS and 60 min mixing than using the 1 ml standard Dynal IMS system. When the sample was mixed for 30 min the performance was 70-fold higher. Also, the FTIMS was 16- and 10-fold better than the 10 ml Dynal IMS separator for 60 and 30 min mixing, respectively.

FTIMS isolation of atoxigenic strains of *E. coli* O157 from 50 ml beef mince homogenate was also performed and shows similar results to those above. Briefly, the FTIMS system produced an 82- and 10-fold improvement in performance compared with the 1 ml standard Dynal IMS and 10 ml Dynal IMS separators.

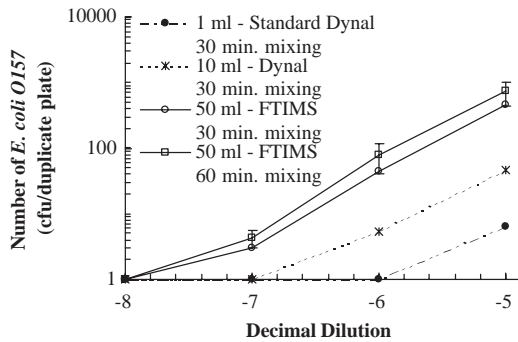


Fig. 6. Recovery of *E. coli* O157 from PBS—FTIMS (volume of cocktail—50 ml and 50  $\mu$ l IDG LabM beads) vs. of 1 ml standard Dynal and 10 ml Dynal systems. The intensity of the magnetic field used with FTIMS was  $H_0 = 640\,000$  A/m and the flow rate was  $Q = 10$  ml/min.

## 6. Conclusions

A large volume FTIMS device has been specified (Table 1) and tested for recovery of MPs—*E. coli* O157 aggregates from PBS and beef mince homogenate samples of 50 ml. The device shows >70 and 10-fold improvements of recovery of *E. coli* O157 compared with standard 1 ml Dynal and 10 ml Dynal separators.

Further experimental validation, for the detection of *E. coli* O157 and other pathogens from different sample matrices is needed. In addition, further improvements are required to simplify the use of the FTIMS apparatus to enable routine application in microbiology laboratories (e.g. ease of multiple sample throughput and sterilisation between samples). Other suitable applications of this technology could involve negative removal of cells or magnetic filtration of carrier particles from body fluids.

## Acknowledgements

This work was funded by EU Marie Curie Fellowship (contract QLK6-CT-2002-51544).

## References

- [1] I. Safarik, M. Safarikova, S.J. Forsythe, *J. Appl. Bacteriol.* 78 (1995) 575.
- [2] I. Safarik, M. Safarikova, *J. Chromatogr. B* 722 (1999) 33.
- [3] A. Thiel, A. Scheffold, A. Rodbruch, *Immunotechnology* 4 (1998) 89.
- [4] N.J.C. Strachan, M. MacRae, N.F. Hepburn, et al., Proceedings of the Fourth International Symposium on Shiga Toxin (Verocytotoxin) Producing *E. coli* Infections, Oct 29—Nov. 2, Kyoto, Japan, 2000, p. 87.
- [5] D.J. Wright, P.A. Chapman, C.A. Siddons, *Epidemiol. Infect.* 113 (1994) 31.
- [6] I.D. Ogden, N. Hepburn, M. MacRae, et al., *Lett. Appl. Microbiol.* 31 (2000) 338.
- [7] V. Badescu, V. Murariu, O. Rotariu, et al., *Powder Technol.* 90 (1997) 131.
- [8] N. Rezlescu, V. Murariu, O. Rotariu, et al., *Powder Technol.* 83 (1995) 259.
- [9] J.H.P. Watson, *J. Appl. Phys.* 44 (1973) 4209.
- [10] R.P.A.R. van Kleef, Particle behaviour in high field magnetic flocculation and separation, Ph.D. Thesis, 1984, p. 51.
- [11] B.I. Bleaney, B. Bleaney, *Electricity and Magnetism*, Oxford University Press, London, 1976, p. 170.
- [12] E. Luca, Gh. Călugăru, R. Bădescu, et al., *Ferrofluids and their industrial applications (Romanian version—"Fero-fluidele și aplicațiile lor industriale")* (Editura Tehnică, București, 1978) p. 68.
- [13] W.H. Press, S.A. Teukolsky, W.T. Vetterling, et al., *Numerical Recipes in Fortran. The Art of Scientific Computing*, second ed., Cambridge University Press, New York, 1992, p. 704.
- [14] I.J. Bousfield, J.L. Smith, R.W. Trueman, *J. Appl. Bacteriol.* 36 (1973) 297.